

Physiologically-Based Pharmacokinetic Modeling to Predict the Clinical Efficacy of the Coadministration of Lopinavir and Ritonavir against SARS-CoV-2

Aarzoo Thakur^{1,2,†}, Shawn Pei Feng Tan^{1,2,†} and James Chun Yip Chan^{1,2,3,*}

Lopinavir/ritonavir, originally developed for treating HIV, is currently undergoing clinical studies for treating the severe acute respiratory syndrome coronavirus 2 (SARS-CoV-2). Although recent reports suggest that lopinavir exhibits *in vitro* efficacy against SARS-CoV-2, it is a highly protein-bound drug and it remains unknown if it reaches adequate *in vivo* unbound (free) concentrations in lung tissue. We built a physiologically-based pharmacokinetic model of lopinavir/ritonavir in white and Chinese populations. Our aim was to perform pharmacokinetic/pharmacodynamic correlations by comparing simulated free plasma and lung concentration values achieved using different dosing regimens of lopinavir/ritonavir with unbound half-maximal effective concentration ($EC_{50,unbound}$) and unbound effective concentration 90% values of lopinavir against SARS-CoV-2. The model was validated against multiple observed clinical datasets for single and repeated dosing of lopinavir/ritonavir. Predicted pharmacokinetic parameters, such as the maximum plasma concentration, area under the plasma concentration-time profile, oral clearance, half-life, and minimum plasma concentration at steady-state were within two-fold of clinical values for both populations. Using the current lopinavir/ritonavir regimen of 400/100 mg twice daily, lopinavir does not achieve sufficient free lung concentrations for efficacy against SARS-CoV-2. Although the Chinese population reaches greater plasma and lung concentrations as compared with whites, our simulations suggest that a significant dose increase from the current clinically used dosing regimen is necessary to reach the $EC_{50,unbound}$ value for both populations. Based on safety data, higher doses would likely lead to QT prolongation and gastrointestinal disorders (nausea, vomiting, and diarrhea), thus, any dose adjustment must be carefully weighed alongside these safety concerns.

Study Highlights

WHAT IS THE CURRENT KNOWLEDGE ON THE TOPIC?

Recent reports indicate that lopinavir inhibits the *in vitro* replication of severe acute respiratory syndrome coronavirus 2 (SARS-CoV-2) but it is uncertain if lopinavir exhibits clinical efficacy. We developed a physiologically-based pharmacokinetic (PBPK) model to predict unbound lung tissue concentrations of lopinavir when co-administered with ritonavir.

WHAT QUESTION DID THIS STUDY ADDRESS?

We aimed to determine (1) if the recommended dose of 400/100 mg of lopinavir/ritonavir twice daily reaches effective unbound lung concentrations necessary for inhibition of SARS-CoV-2; (2) the optimal dosing regimens required in both

white and Chinese populations; and (3) whether this optimal dosing regimen is clinically safe.

WHAT DOES THIS STUDY ADD TO OUR KNOWLEDGE?

The recommended dose for lopinavir/ritonavir does not reach therapeutic unbound lung concentrations against SARS-CoV-2. A significantly larger loading and maintenance dose is necessary but may pose safety concerns.

HOW MIGHT THIS CHANGE CLINICAL PHARMACOLOGY OR TRANSLATIONAL SCIENCE?

Our study exemplifies the utility of PBPK modeling to predict tissue concentrations for building pharmacokinetic/pharmacodynamic (PK/PD) correlations of drugs and the need to account for the free fraction of drugs when making PK/PD assessments.

¹Innovations in Food and Chemical Safety, Agency for Science, Technology, and Research, Singapore City, Singapore; ²Skin Research Institute of Singapore, Agency for Science, Technology, and Research, Singapore City, Singapore; ³Singapore Institute of Food and Biotechnology Innovation, Agency for Science, Technology, and Research, Singapore City, Singapore. *Correspondence: James Chun Yip Chan (james_chan@sifbi.a-star.edu.sg)

[†]These authors should be considered joint first authors.

Received April 20, 2020; accepted July 28, 2020. doi:10.1002/cpt.2014

On December 31, 2019, China notified the World Health Organization (WHO) regarding multiple cases of pneumonia in Wuhan, China. Today, this pneumonia is known as coronavirus disease 2019 (COVID-19) and has been found to be caused by the severe acute respiratory syndrome coronavirus 2 (SARS-CoV-2) virus leading to over 11.1 million positive cases and 528,000 deaths worldwide as of July 5, 2020.¹ Repurposing existing drugs with proven human safety profiles is expected to provide an expedited route to rapidly identify effective pharmacotherapy against SARS-CoV-2. One therapy currently of high interest is lopinavir/ritonavir, a protease inhibitor therapy initially approved for the treatment of the human immunodeficiency virus (HIV).² This combination has attracted attention because of a long history of use, wide availability, and evidence of efficacy against other coronaviruses, such as Middle East respiratory syndrome coronavirus (MERS-CoV) and SARS-CoV-1.^{3,4} Lopinavir/ritonavir was tested in clinical trials globally through the SOLIDARITY trial conducted by the WHO and there are many instances of off-label, compassionate use by physicians to treat COVID-19.⁵ Despite widespread use, there is little evidence available in the literature to support its antiviral activity against SARS-CoV-2. In particular, Cao *et al.* reported that a recent randomized control trial on 199 critical patients with COVID-19 did not demonstrate significant clinical improvement in those receiving 400/100 mg lopinavir/ritonavir twice daily for 14 days over standard of care.⁶ We hypothesized that one possible explanation for the lack of efficacy reported by Cao *et al.* could be insufficient unbound (free) concentrations of lopinavir in lung tissue ($C_{u, \text{lung}}$) achieved by the dosing regimen used in the study.

To address this possibility, we utilized physiologically-based pharmacokinetic (PBPK) modeling to simulate the $C_{u, \text{lung}}$ of lopinavir achieved by 400/100 mg twice daily dose of lopinavir/ritonavir in both white and Chinese populations. Lopinavir (victim drug) exhibits complex drug-drug interactions (DDIs) with ritonavir (perpetrator drug), with cytochrome P450 (CYP450) mediated mechanism-based inactivation (MBI) dominating initially, followed by induction.⁷ Although a minimal PBPK model was previously reported for lopinavir/ritonavir,⁸ it did not recapitulate the pharmacokinetic (PK) profile of the single dose administration of 400/100 mg lopinavir/ritonavir, as the model was optimized for a repeated dosing regimen. Furthermore, the use of an empirical additional clearance component for the elimination of ritonavir, which in turn exerts a major influence on the systemic exposure of lopinavir, limited its mechanistic extrapolation to other populations (e.g., ethnic Han Chinese) with lower CYP450 enzyme expression levels.^{9,10} Separately, a population PK model by Aspiroz *et al.*¹¹ was recently utilized by Smith *et al.*¹² to simulate the concentrations of lopinavir in plasma and lung and compared them with half-maximal effective concentration (EC_{50}) values of lopinavir against HIV, SARS-CoV, and MERS-CoV. However, it was a top-down model and included an empirical time-varying lopinavir clearance in order to simulate the effects of simultaneous inactivation and induction on steady-state levels. This top-down approach would similarly limit mechanistic extrapolation to other populations.

Using over 40 sets of *in vitro* data, we built and rigorously validated a middle-out, full PBPK model for lopinavir alone, and

lopinavir/ritonavir using the Simcyp Simulator. The model was used to predict $C_{u, \text{lung}}$ derived from human lung tissue-to-plasma partition coefficient ($K_{p, \text{lung}}$) values. As lopinavir is highly protein bound, the free fraction of lopinavir available to interact with pharmacological targets in human tissue and plasma is low.¹³ Such considerations influence the free fraction of lopinavir in *in vitro* assays, which in turn affects potency measurements.^{14,15} Therefore, we derived unbound EC_{50} ($EC_{50, \text{unbound}}$) values against SARS-CoV-2 from various literature reports and compared it against the predicted $C_{u, \text{lung}}$ values to determine if clinically used doses of 400/100 mg twice a day would reach efficacious lung concentrations in white and Chinese populations.^{16,17} Subsequently, we predicted the optimal dosing regimens required to reach the efficacious lung concentrations in both populations.

METHODS

BPBK model development

Middle-out BPBK models of lopinavir and ritonavir were built using population-based Simcyp Simulator version 19 (Certara, Simcyp Division, Sheffield, UK). In particular, a perfusion-limited full BPBK distribution model was implemented to permit prediction of tissue concentrations. For lopinavir, tissue K_p values were predicted using the corrected Poulin and Thiel approach (method 1), except for human $K_{p, \text{lung}}$, which was calculated from experimental values of unbound lopinavir fraction in lung ($f_{u, \text{lung}}$) and plasma ($f_{u, \text{p}}$).¹⁸ The hepatic metabolism of lopinavir by CYP3A4 was accounted for using microsomal kinetic parameters,² whereas the maximal inactivation rate constant for MBI of CYP3A4 by lopinavir was optimized according to Wagner *et al.*⁸ For ritonavir, extensive metabolic kinetic parameters from recombinant CYP enzymes were coupled with intersystem extrapolation factors and incorporated into the model to account for its hepatic metabolism.^{19,20} Subsequently, lopinavir (substrate) and ritonavir (inhibitor) models were linked. Experimental values for MBI and induction of CYP3A4 by ritonavir were used to define the complex time-dependent inhibition and induction of lopinavir metabolism by ritonavir.²¹ Finally, an active hepatic scalar was empirically fitted to achieve an optimal induction of lopinavir metabolism. All the drug-specific parameters of lopinavir and ritonavir are listed in **Table S1**.

Model validation

Simulations were performed for an oral administration of single dose of lopinavir 400 mg, single dose of lopinavir/ritonavir 400/100 mg, and repeated dosing of 400/100 mg twice daily regimen for white and Chinese populations using the Simcyp Healthy Volunteers and Chinese Healthy Volunteers population database, respectively. Simulated results were visually inspected by overlaying clinical plasma concentration-time profiles (extracted using WebPlotDigitizer, San Francisco, CA) with model predictions.^{2,22–28} Thereafter, the PBPK models were validated using a two-fold criterion to compare the clinically observed and model predicted PK parameters, such as the maximum plasma concentration (C_{max}), area under the plasma concentration-time profile (AUC_{0-t}), time needed to reach C_{max} (T_{max}), oral clearance (CL/F), terminal half-life, and minimum plasma concentration at steady-state (C_{min}).

Assessing pharmacodynamic efficacy against HIV and SARS-CoV-2

Once the PBPK model was validated, it was first used to assess lopinavir's efficacy against HIV by comparing its unbound concentrations in white blood cells ($C_{u, \text{WBC}}$) with $EC_{50, \text{unbound}}$ value against HIV-infected lymphocytes. This was done to verify that the current PBPK model is able to recapitulate the clinical efficacy of lopinavir against HIV. Likewise, the pharmacodynamic (PD) assessment against SARS-CoV-2 was performed by predicting if lopinavir reaches therapeutic

concentrations in the lung, $C_{u,\text{lung}}$ was compared with the $EC_{50,\text{unbound}}$ and $EC_{90,\text{unbound}}$ values of lopinavir against SARS-CoV-2-infected Vero E6/TMPRSS2 cells, respectively.^{16,17} Because lopinavir is a poor substrate of uptake or efflux transporters and its cellular entry occurs passively,^{29,30} it follows the free drug hypothesis. Accordingly, at steady-state, free concentration of lopinavir is the same on both sides of any biomembrane.³¹ Therefore, $C_{u,\text{WBC}}$ and $C_{u,\text{lung}}$ were calculated using Eq. 1:

$$C_{u,\text{tissue}} = C_{\text{plasma}} \times f_{u,p} = C_{\text{tissue}} \times f_{u,\text{tissue}} \quad (1)$$

where, $C_{u,\text{tissue}}$ represents the unbound tissue concentration; C_{plasma} and C_{tissue} are the total plasma and tissue concentrations, respectively; and $f_{u,\text{tissue}}$ is the unbound fraction in tissues. As the Simcyp model does not possess a white blood cell (WBC) compartment, $C_{u,\text{WBC}}$ was assumed to be the same as $C_{u,\text{plasma}}$. $C_{u,\text{lung}}$ was calculated based on simulated total lung concentrations (C_{lung}) and experimental $f_{u,\text{lung}}$ measurements.

The $EC_{50,\text{unbound}}$ value against HIV was obtained from literature.¹⁵ $EC_{50,\text{unbound}}$ and $EC_{90,\text{unbound}}$ values against SARS-CoV-2 were not readily available and had to be calculated as the product of EC_{50} or EC_{90} values reported by Ohashi *et al.* and Yamamoto *et al.*,^{16,17} and the free fraction of lopinavir in fetal calf serum (FCS) culture media ($f_{u,\text{media}}$) obtained from Hickman *et al.*¹⁵ As Hickman *et al.* reported the free fractions of 1 $\mu\text{g/mL}$ lopinavir in 5–50% FCS containing media, this was used to model the relationship between FCS content in media and $f_{u,\text{media}}$, to obtain the free fraction in 2% FCS (used by Ohashi *et al.*).¹⁷ Yamamoto *et al.* used 5% FCS in their culture media.¹⁶ The model is defined by Eq. 2:

$$f_u = \frac{1}{1 + K_a \times f_{u,\text{prot}} \times P_t} \quad (2)$$

where, K_a is the association constant, $f_{u,\text{prot}}$ represents the fraction of unoccupied protein sites, and P_t is the total protein concentration. Keeping the product of K_a and $f_{u,\text{prot}}$ constant, Eq. 2 was analyzed using Graphpad Prism 8 (GraphPad Software, La Jolla, CA) to determine the $f_{u,\text{media}}$ in 2% FCS. The impact of protein binding on PK/PD assessments were then assessed by comparing the predicted total and unbound lung concentrations of 400/100 mg twice daily lopinavir/ritonavir with EC_{50} and $EC_{50,\text{unbound}}$ values of lopinavir against SARS-CoV-2, respectively.

Dose optimization for SARS-CoV-2 therapy

In both white and Chinese populations, simulations were performed with gradually increasing combinations of loading and maintenance doses in order to reach $C_{u,\text{lung}}$ values comparable with $EC_{50,\text{unbound}}$ and $EC_{90,\text{unbound}}$ values of lopinavir against SARS-CoV-2. The optimal dose was determined when the steady-state unbound lung C_{max} reached the $EC_{50,\text{unbound}}$ value.

RESULTS

BPBK model validation in white and Chinese populations

Simulated plasma concentration-time profiles for single and repeated twice daily doses of 400/100 mg lopinavir/ritonavir in white and Chinese populations are shown in **Figure 1a-c**. Clinically observed and model predicted PK parameters were compared and the fold difference values were within the two-fold criterion (**Tables 1–3**). After a single dose of lopinavir before and after the DDI with ritonavir, the predicted CL/F of lopinavir decreased drastically from a mean value of 373.83 L/h to 3.49 L/h due to the profound inhibition of CYP3A4 by ritonavir. CL/F of lopinavir was variable, depending on the duration of lopinavir/ritonavir therapy and the population as

well. After repeated dosing of lopinavir/ritonavir, the predicted mean CL/F in white healthy volunteers increased to 6.02 L/h due to the induction of CYP3A4 by ritonavir. The predicted CL/F after repeated dosing in white healthy volunteers were greater than the Chinese populations (3.81 L/h), corresponding with observed clinical data.^{2,22,25} Predicted C_{max} and AUC_{0-t} were in turn greater in Chinese (20.00 $\mu\text{g/mL}$ and 204.29 $\mu\text{g/mL}\cdot\text{h}$) in comparison to white healthy volunteers (13.02 $\mu\text{g/mL}$ and 117.68 $\mu\text{g/mL}\cdot\text{h}$).

Assessing efficacy against HIV and SARS-CoV-2 at clinical doses

The predicted lopinavir $C_{u,\text{WBC}}$ after twice daily dosing of 400/100 mg lopinavir/ritonavir in both white and Chinese populations were 100-fold higher than the $EC_{50,\text{unbound}}$ value of lopinavir against HIV ($0.00069 \pm 0.00006 \mu\text{g/mL}$).¹⁵ The concentration-time profiles along with $EC_{50,\text{unbound}}$ values are shown in **Figure 1d,e**. The $f_{u,\text{media}}$ for lopinavir in 2% FCS was determined to be 0.355, which yielded an $EC_{50,\text{unbound}}$ value of 0.386 $\mu\text{g/mL}$ and $EC_{90,\text{unbound}}$ value of 0.806 $\mu\text{g/mL}$ against SARS-CoV-2 from Ohashi *et al.*,¹⁷ whereas the corresponding $f_{u,\text{media}}$ in 5% FCS was reported by Hickman *et al.* as 0.200, which yielded an $EC_{50,\text{unbound}}$ value of 0.721 $\mu\text{g/mL}$ from Yamamoto *et al.*¹⁶ Using the same dosing regimen, a comparison of the $C_{u,\text{lung}}$ with both $EC_{50,\text{unbound}}$ and $EC_{90,\text{unbound}}$ values of lopinavir against SARS-CoV-2 showed that insufficient unbound lopinavir concentrations were achieved in lung tissue for both white (unbound lung $C_{\text{max}} = 0.130 \mu\text{g/mL}$) and Chinese populations (unbound lung $C_{\text{max}} = 0.200 \mu\text{g/mL}$; **Figure 2a,b**).

As protein binding has a major impact on both unbound tissue concentrations and *in vitro* $EC_{50,\text{unbound}}$ values, we compared the juxtaposition of both total and unbound values at steady-state after twice daily dose of 400/100 mg lopinavir/ritonavir in white populations (**Figure 2c**). The total lung C_{min} (15.72 $\mu\text{g/mL}$) was ~ 15 -fold greater than EC_{50} value of lopinavir from Ohashi *et al.* (1.09 $\mu\text{g/mL}$). However, the same was not true for comparison of unbound values. $C_{u,\text{lung}}$ (a function of both plasma and tissue binding) was lower than the $EC_{50,\text{unbound}}$ value of lopinavir (a function of binding to protein within the incubation media).

Dose optimization for SARS-CoV-2 therapy

Different combinations of loading and maintenance doses of lopinavir/ritonavir were trialed to simulate $C_{u,\text{lung}}$ values, beginning with the 400/100 mg twice daily regimen currently tested in clinical trials (**Figure 2d**). The predicted unbound lung PK parameters are listed in **Table 4**. In the white population, 2 hypothetical loading doses of 1,600/400 mg followed by a maintenance dose of 1,400/350 mg lopinavir/ritonavir twice daily was needed to achieve sufficient free lung concentration at steady state (unbound lung $C_{\text{max}} = 0.414 \mu\text{g/mL}$) matching the lowest $EC_{50,\text{unbound}}$ value (0.386 $\mu\text{g/mL}$) reported by Ohashi *et al.* In the Chinese population, this was achieved with 2 loading doses of 1,200/300 mg followed by twice daily dosing of 1,000/250 mg lopinavir/ritonavir (unbound lung $C_{\text{max}} = 0.479 \mu\text{g/mL}$).

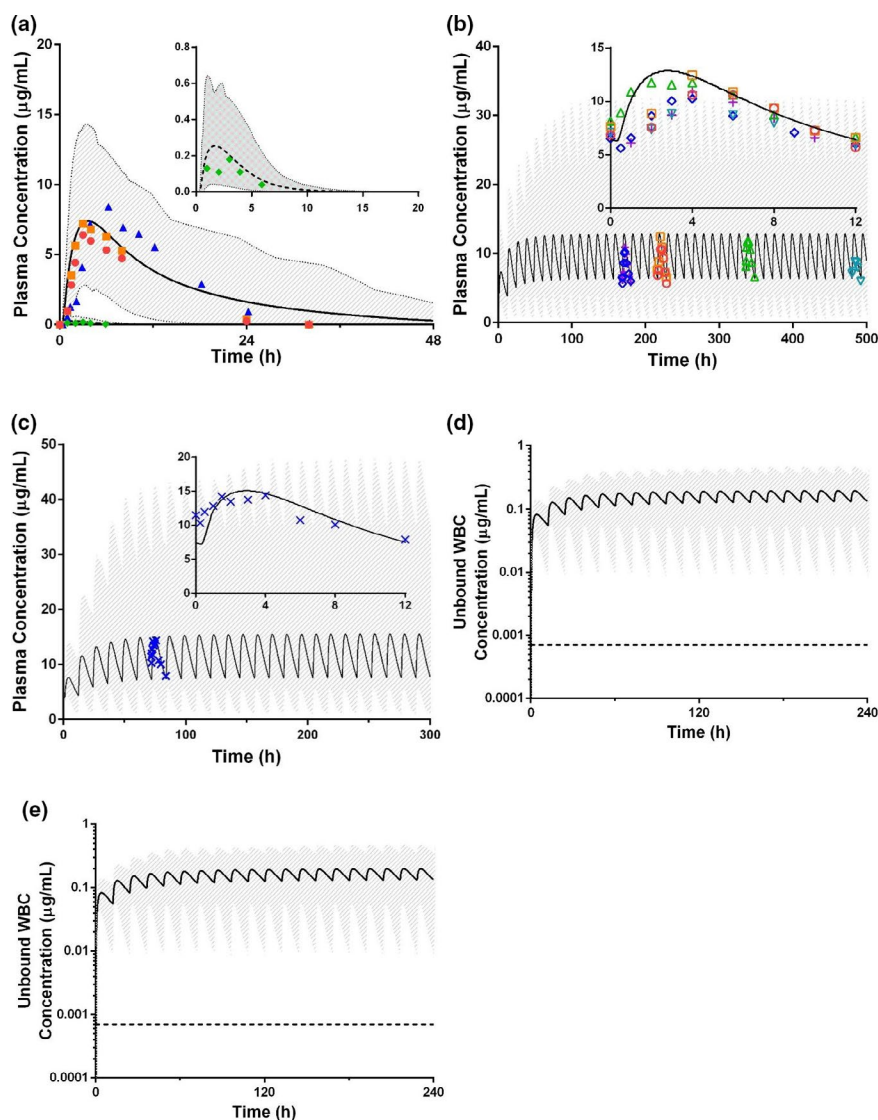


Figure 1 Simulated lopinavir plasma concentration-time profile in (a) White healthy volunteers after a single oral dose of lopinavir/ritonavir 400/100 mg with the inset describing the plasma concentrations of lopinavir 400 mg alone and in (b) white and (c) Chinese populations after repeated oral dose of lopinavir/ritonavir 400/100 mg twice a day with the inset describing a combined overlay of the steady-state predicted plasma concentration profile with observed clinical data points extracted from studies giving steady-state measurements. Simulated unbound lopinavir white blood cell (WBC) concentration-time profiles in (d) white healthy volunteers and (e) Chinese patients after repeated oral doses of lopinavir/ritonavir 400/100 mg twice daily. The solid black lines represent the simulated mean lopinavir concentrations with the 95th and 5th percentile of population levels bounded by the grey shaded area, whereas the dashed line represents the $EC_{50,unbound}$ value against HIV. The symbols (\blacktriangle^2 , \blacklozenge^2 , \blacksquare^{28} , \bullet^{28} , \square^{22} , \circ^{22} , \diamond^{23} , \triangle^{26} , ∇^{27} , $+^{24}$, \times^{25}) represent the reported clinical data.

DISCUSSION

With the rapidly evolving COVID-19 crisis worldwide and the urgent need for effective pharmacotherapy against SARS-CoV-2, repurposing of existing drugs with proven human safety profiles provide an expedited route to effective treatment. This requires correlating the unbound lung concentrations with PD measurements, such as *in vitro* $EC_{50,unbound}$ values for inhibition of viral replication. As only the free drug is available to engage its pharmacological target, such PK/PD correlations require comparison of unbound tissue concentrations with unbound *in vitro* dose-response assessments. This is a crucial, but often neglected consideration, particularly for highly protein-bound drugs. Despite widespread clinical use, it remains unclear if the current dosing

therapy of 400/100 mg lopinavir/ritonavir twice daily achieves efficacious lung concentrations against SARS-CoV-2. The presence of lopinavir in fluid and cells obtained from bronchoalveolar lavage of HIV-infected patients receiving lopinavir/ritonavir indicate the possibility of lung penetration.^{32,33} Despite this evidence, a recently published clinical study reported that 400/100 mg lopinavir/ritonavir did not demonstrate a statistically significant benefit vs. standard of care in critical patients with COVID-19.⁶ Determination of free lung concentrations of lopinavir could explain the observed failure of therapy. However, *in vivo* measurements of free lung concentrations are invasive and difficult to obtain, hence PBPK modeling is a useful tool to obtain such information.³⁴

Table 1 Predicted vs. observed pharmacokinetic parameters of lopinavir after a single oral dose of lopinavir 400 mg and lopinavir/ritonavir 400/100 mg in the white population

PK parameter	Predicted			Observed		
	Mean	Geo. mean	Median	Study 1 ² Mean	Study 2 ²⁸ Median	Study 2 Median
Lopinavir alone						
C _{max} , µg/mL	0.26	0.17	0.16	0.19	–	–
P/O ratio				1.37	–	–
AUC _{0–t} , µg/mL.h	1.07	0.67	0.68	0.67	–	–
P/O ratio				1.60	–	–
T _{max} , hours	1.65	1.60	1.61	2.30	–	–
P/O ratio				0.72	–	–
CL/F, L/h	373.83	597.01	588.24	597.01	–	–
P/O ratio				0.63	–	–
Lopinavir/ritonavir coadministration						
C _{max} , µg/mL	7.72	6.80	7.06	8.5	7.2	6.5
P/O ratio				0.91	0.98	1.09
AUC _{0–t} , µg/mL.h	114.77	84.22	90.65	105.3	71.8	58.7
P/O ratio				1.09	1.26	1.54
T _{max} , hours	3.97	3.80	3.83	5.2	–	–
P/O ratio				0.76	–	–
CL/F, L/h	3.49	4.75	4.41	3.80	5.57	6.81
P/O ratio				0.92	0.79	0.65

P/O ratio represents the fold-difference between predicted vs. observed value. CL/F was calculated by taking lopinavir dose of 400 mg divided by the corresponding AUC_{0–t}.

AUC_{0–t}, area under the plasma concentration-time profile; CL/F, oral clearance; C_{max}, maximum plasma concentration; PK, pharmacokinetic; T_{max}, time to maximum plasma concentration.

Using a linked full PBPK model of lopinavir and ritonavir, we were able to robustly recapitulate the AUC_{0–t}, C_{max}, C_{min}, and CL/F of lopinavir after a single and repeated twice daily dosing

of 400/100 mg lopinavir/ritonavir in the white population. The PBPK model was able to accurately predict the increase in lopinavir's C_{max} and AUC_{0–t} after a single dose of lopinavir before and

Table 2 Predicted vs. observed pharmacokinetic parameters of lopinavir after a repeated oral dose of lopinavir/ritonavir 400/100 mg twice a day in the white population at steady-state

PK Parameter	Predicted			Observed								
	Mean	Geo. Mean	Median	Study 1 ² Mean	Study 1 Mean	Study 1 Mean	Study 2 ²² Mean	Study 2 Mean	Study 3 ²³ Mean	Study 4 ²⁷ Mean	Study 5 ²⁶ Geo. Mean	Study 6 ²⁴ Geo. Mean
C _{max} , µg/mL	13.02	10.83	10.92	9.58	10.36	9.58	12.9	12.3	11.17	9.81	11.90	11.97
P/O ratio	–	–	–	1.36	1.26	1.36	1.01	1.06	1.17	1.33	0.91	0.91
AUC _{0–t} , µg/mL.h	117.68	88.29	89.16	82.8	87.8	88.2	111.8	102.9	96.79	92.60	109	99.60
P/O ratio	–	–	–	1.42	1.34	1.33	1.05	1.14	1.22	1.27	0.81	0.89
C _{min} , µg/mL	6.18	3.21	3.77	–	4.66	5.31	6.5	5.2	5.33	5.51	–	5.78 ^a
P/O ratio	–	–	–	–	1.33	1.16	0.95	1.19	1.16	1.12	–	0.56
CL/F, L/h	6.02	4.53	4.49	6.4	–	–	4.24	4.52	–	–	3.66	–
P/O ratio	–	–	–	0.94	–	–	1.42	1.33	–	–	1.24	–
t _{1/2} , hours	8.06	6.43	6.48	–	5.76	–	6.8	6.2	–	–	8.7	–
P/O ratio	–	–	–	–	1.4	–	1.19	1.3	–	–	0.74	–

P/O ratio represents the fold-difference between predicted vs. observed values.

CL/F, oral clearance; C_{max}, peak plasma concentration; C_{min}, minimum plasma concentration at steady-state; t_{1/2}, terminal half-life.

^aC_{trough} reported instead of C_{min}.

Table 3 Predicted vs. observed pharmacokinetic parameters of lopinavir after a repeated oral dose of lopinavir/ritonavir 400/100 mg twice a day in Chinese population at day 4 and steady-state

PK Parameter	Predicted – Day 4			Predicted – Steady State			Observed – Day 4 ²⁵ Geo. Mean
	Mean	Geo. Mean	Median	Mean	Geo. Mean	Median	
C _{max} , µg/mL	18.48	15.20	14.34	20.00	15.72	14.39	15.29
P/O ratio	–	–	–	–	–	–	0.99
AUC _{0-t} , µg/mL.h	186.91	142.18	141.40	204.29	147.08	142.08	134.70
P/O ratio	–	–	–	–	–	–	1.06
C _{min} , µg/mL	–	–	–	13.12	7.37	8.28	11.45
P/O ratio	–	–	–	–	–	–	0.64 ^a
CL/F, L/h	–	–	–	3.81	2.72	2.82	3.46
P/O ratio	–	–	–	–	–	–	0.79 ^a
t _{1/2} , hours	–	–	–	13.81	10.61	10.68	12.33
P/O ratio	–	–	–	–	–	–	0.86 ^a

P/O ratio represents the fold-difference between predicted vs. observed value.

CL/F, oral clearance; C_{max}, peak plasma concentration; C_{min}, minimum plasma concentration at steady-state; PK, pharmacokinetic.

^aPredicted steady-state values were used to obtain the P/O ratio.

after the DDI with ritonavir, illustrating the rapid inhibition of lopinavir's metabolism by ritonavir. The subsequent induction of CYP3A4 by ritonavir after repeated dosing of lopinavir/ritonavir was recapitulated by the increase in lopinavir's CL/F moving from single to multiple doses. The mechanistic model also permitted extrapolation to the Chinese population, and here we demonstrate that the model recovered the observed lower CL/F and greater terminal half-life in the Chinese subjects, which can be attributed to a smaller liver volume and lower abundance of CYP enzymes in the liver.⁹

Lopinavir is a perfusion-limited drug and is neither dependent on transporters for pulmonary entry nor undergoes elimination in the lung. Additionally, it is a neutral compound and does not accumulate in the tissues due to pH-driven partitioning. Therefore, the unbound plasma concentrations can be regarded to be equivalent to unbound tissue concentrations. Based on these observations, we simulated the unbound concentrations of lopinavir in WBCs and lung tissue and juxtaposed these simulations against EC_{50,unbound} values for inhibition of HIV and SARS-CoV-2 replication. The C_{u,WBC} was compared with EC_{50,unbound} values against HIV to demonstrate that the current PBPK model can be extrapolated to make PD predictions. For inhibition of HIV, the model predicted C_{u,WBC} values were 100-fold higher than EC_{50,unbound} values in HIV-infected WBCs. Because lopinavir/ritonavir is clinically efficacious against HIV treatment, the ability of the present model to recapitulate this efficacy through PK/PD correlation builds confidence both in the model and our approach. The robust PK/PD correlation of lopinavir/ritonavir for HIV treatment suggested the possibility of a similar evaluation of therapeutic efficacy in the context of SARS-CoV-2.

Currently, to our knowledge, there are four reports of EC₅₀ values of lopinavir against SARS-CoV-2,^{16,17,35,36} that exhibit high variability (15-fold difference) in the *in vitro* values. Of these, we utilized data from two reports, Ohashi *et al.* and Yamamoto *et al.* (extracted from pre-print manuscripts) to derive EC_{50,unbound} values. Such potency values are influenced by several experimental factors,

including host cell choice, multiplicity of infection, infection and treatment sequences, treatment duration, and readout method. Although Ohashi *et al.* and Yamamoto *et al.* determined EC₅₀ values using Vero E6 cells expressing the TMPRSS2 serine protease, the remaining studies used unmodified Vero E6 and unmodified Vero cells respectively for EC₅₀ measurements.^{35,36} Current evidence indicates that SARS-CoV-2 utilizes the TMPRSS2 protease for viral spike protein priming, which is necessary for SARS-CoV-2 viral entry.³⁷ Furthermore, it has been found that the SARS-CoV-2 RNA copies in the Vero E6/TMPRSS2 cell culture supernatants were > 100 times greater than those from Vero E6 cells.³⁸ Thus, the Vero E6/TMPRSS2 cell system is more robust, sensitive, and well-suited for performing *in vitro* efficacy measurements of pharmaceutical compounds against SARS-CoV-2, and here we utilized the EC₅₀ values obtained from such cell systems.

Understanding the free/unbound drug concentration at the target site is critical as it is the free drug that exerts its pharmacological action.³¹ In white populations, comparison of the predicted total and unbound lung concentration of lopinavir (on administration of twice daily 400/100 mg lopinavir/ritonavir) with its EC₅₀ and EC_{50,unbound} against SARS-CoV-2 yield contrasting results. Even though the total lung concentration was greater than the EC₅₀, when *in vivo* and *in vitro* protein binding were used to correct the corresponding lopinavir concentrations, the opposite trend is observed; where C_{u,lung} is now lower than EC_{50,unbound},⁹ indicating a lack of efficacy. This highlights the importance of accounting for the free fraction of a drug, both *in vivo* and *in vitro*, in performing PK/PD correlation and assessing efficacy particularly for highly protein-bound drugs.

Our simulations show that none of the EC_{50,unbound} values are reached by the C_{u,lung} when 400/100 mg twice daily dosing is administered to either white or Chinese populations. Therefore, it is plausible that the failure of a 400/100 mg twice daily regimen for COVID-19 reported by Cao *et al.*⁶ could be due to insufficient free lung concentrations. During the writing of this manuscript, the WHO announced their decision to discontinue the lopinavir/

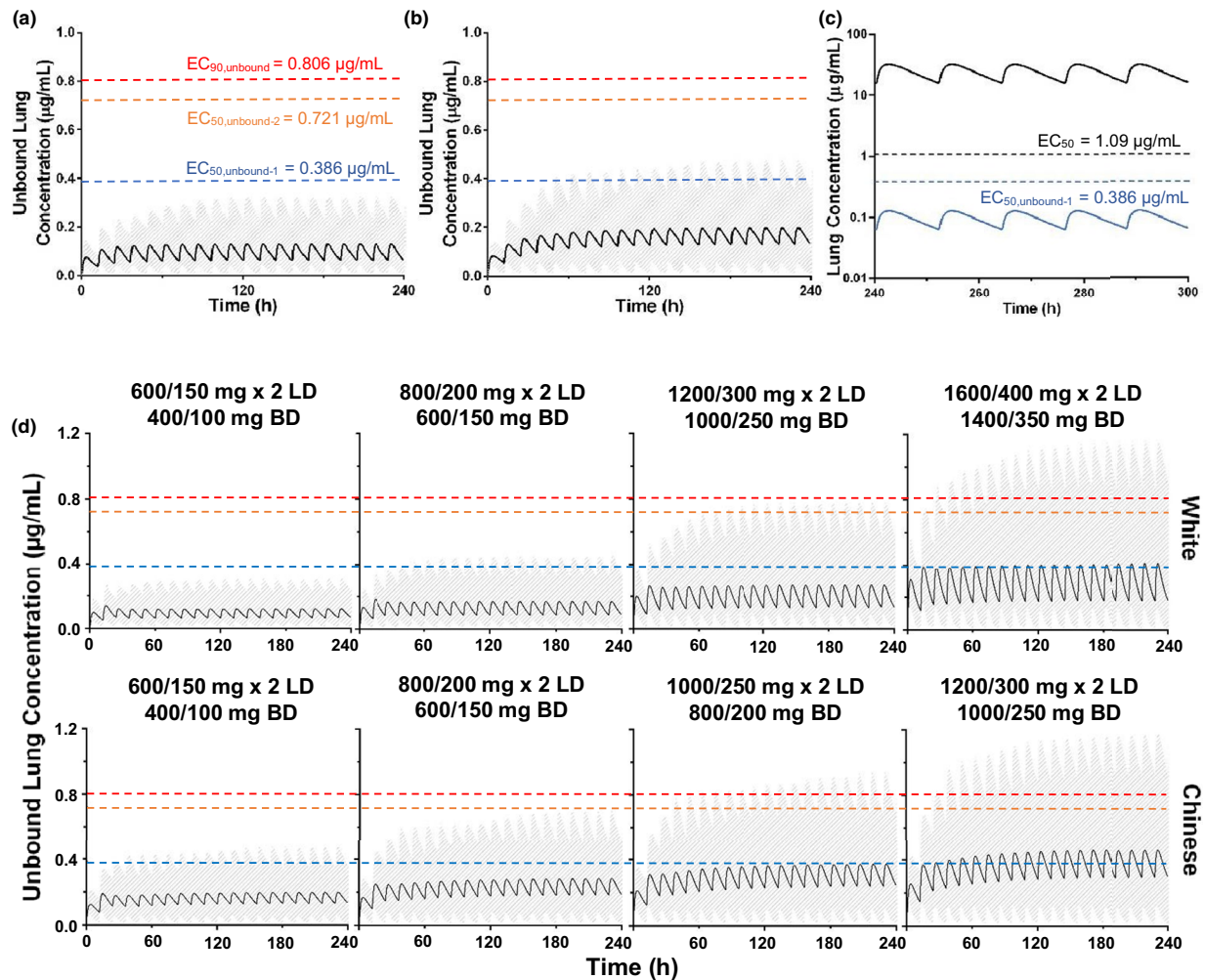


Figure 2 Simulated lopinavir unbound lung concentration-time profiles in (a) White healthy volunteers and (b) Chinese patients after repeated doses of lopinavir/ritonavir 400/100 mg twice daily. (c) Comparison of lopinavir total and unbound lung concentration-time profiles in white healthy volunteers after repeated doses of lopinavir/ritonavir 400/100 mg twice daily. (d) Simulated lopinavir unbound lung concentration-time profiles in both white healthy volunteers and Chinese patients after various dosing regimens. The solid black line represents the simulated mean lopinavir unbound lung concentrations (a, b, d) with the 95th and 5th percentile of population levels bounded by the grey shaded area, whereas the dashed blue and red lines represent unbound half-maximal effective concentration ($EC_{50,unbound-1}$) and $EC_{90,unbound}$ values against severe acute respiratory syndrome coronavirus 2 (SARS-CoV-2) from Ohashi *et al.*¹⁷ and the dashed orange line represents the $EC_{50,unbound-2}$ value against SARS-CoV-2 from Yamamoto *et al.*¹⁶ In (c), solid black and blue lines represent lopinavir total and unbound lung concentrations, respectively, while the dashed black and blue lines represent EC_{50} and $EC_{50,unbound-1}$ values against SARS-CoV-2 from Ohashi *et al.*, respectively.¹⁷ LD and BD refer to loading dose and twice daily dosing, respectively.

Table 4 Predicted mean pharmacokinetic parameters of unbound lopinavir in the lungs after increasing doses of lopinavir/ritonavir in white and Chinese populations at steady-state

Loading dose, mg	Maintenance dose, mg	White			Chinese		
		C_{max} , µg/mL	C_{min} , µg/mL	AUC_{0-t} , µg/mL.h	C_{max} , µg/mL	C_{min} , µg/mL	AUC_{0-t} , µg/mL.h
600/150	400/100 BD	0.130	0.062	1.177	0.200	0.131	2.043
800/200	600/150 BD	0.172	0.085	1.577	0.288	0.184	2.908
1,000/250	800/200 BD	0.221	0.106	2.008	0.379	0.240	3.815
1,200/300	1,000/250 BD	0.272	0.128	2.453	0.479	0.301	4.786
1,400/350	1,200/300 BD	0.353	0.148	3.042	–	–	–
1,600/400	1,400/350 BD	0.414	0.174	3.567	–	–	–

BD refers to twice daily dosing.

Two loading doses were administered before the maintenance dosing.

AUC_{0-t} , area under the plasma concentration-time profile; C_{max} , maximum plasma concentration; C_{min} , minimum plasma concentration at steady-state.

ritonavir treatment arm in hospitalized patients with COVID-19 taking part in the SOLIDARITY trials as well.³⁹ A dose adjustment may therefore be necessary to increase free lung concentrations of lopinavir. Our simulations suggest that in the white population, efficacious concentrations can be reached in lung on administration of 2 loading doses of 1,600/400 mg followed by maintenance doses of 1,400/350 mg twice daily lopinavir/ritonavir dose. For Chinese populations, 2 loading doses of 1,200/300 mg followed by maintenance doses of 1,000/250 mg twice daily lopinavir/ritonavir is required. These elevated doses can plausibly reach $C_{u, \text{lung}}$ similar to $EC_{50, \text{unbound}}$ values of lopinavir against SARS-CoV-2.

However, it is imperative to consider the safety of such dose escalations. The elevated doses are several times greater than the clinically used doses. We derived guidance from adverse events observed in two high-dose lopinavir/ritonavir studies. In the study by Podzamczar *et al.*, administration of 667/167 mg twice daily lopinavir/ritonavir for 48 weeks led to elevation in aspartate aminotransferase and/or alanine aminotransferase levels in 3 subjects at an average lopinavir plasma C_{max} of 16.2 $\mu\text{g/mL}$.⁴⁰ In another study by Vicente *et al.*, administration of 800/200 mg twice daily doses of lopinavir/ritonavir for 2.5 days led to a concentration-dependent prolongation of QT interval at the highest achieved plasma C_{max} of 24.3 $\mu\text{g/mL}$ (without Torsades de Pointes).⁴¹ Given that the plasma concentrations needed to reach $EC_{50, \text{unbound}}$ values are higher than this threshold, a dose increase of lopinavir/ritonavir in patients with COVID-19 will be limited by possible cardiotoxicity of the combination. In the results of the clinical trial published by Cao *et al.*, a small proportion of patients with COVID-19 experienced QT prolongation at clinical doses of 400/100 mg twice daily, whereas the most common adverse effects were nausea, vomiting, and diarrhea.⁶ Moreover, SARS-CoV-2 can also adversely affect the heart, either directly by infecting cardiac cells and/or indirectly by inducing a cytokine storm.⁴² Finally, the elevated doses are highly likely to result in gastrointestinal adverse effects, which may be dose-limiting. Therefore, in the absence of efficacy at clinical doses and the presence of safety concerns at higher doses, the utility of lopinavir/ritonavir to treat COVID-19 should be revisited.

Our study has several limitations. First, the $f_{u, \text{lung}}$ value used to predict $K_{p, \text{lung}}$ was determined using tissue homogenate and may not describe the intracellular drug binding accurately.¹⁸ Second, due to limited availability of Chinese PK data, extensive validation of the Chinese model was not possible in the present study. Third, local and systemic inflammation, or mechanical interventions, such as intubation, may modify drug binding, distribution, or clearance in patients with COVID-19. For example, cytokine storms observed in patients with COVID-19 may lead to a suppression of CYP3A enzyme activity, leading to decreased metabolism of lopinavir and greater systemic exposure.⁴³ These factors could not be accounted for in the model. Finally, we utilized measurements of lopinavir's $f_{u, \text{media}}$ from a separate study to derive $EC_{50, \text{unbound}}$. As estimations of $EC_{50, \text{unbound}}$ is sensitive to the value of $f_{u, \text{media}}$, and $f_{u, \text{media}}$ in turn, depends on the concentration of the drug, composition of the incubation media, and reagents used, our estimations of $EC_{50, \text{unbound}}$ may not be definitive. We recommend that future *in vitro* PD assessments of drugs known to have high

protein binding should be accompanied with parallel measurements of $f_{u, \text{media}}$.

With a number of clinical trials investigating the efficacy of lopinavir/ritonavir,⁴⁴ it is critical to highlight that the current dosing regimen may be ineffective pertaining to insufficient lung concentrations of lopinavir. The current work shows that presence of efficacy in *in vitro* models may not translate into *in vivo* efficacy. It can occur due to a PK/PD disconnect as a result of inadequate free drug concentration at the site of action. This PK/PD correlation is an important aspect of drug repurposing and should be assessed prior to clinical trials using PBPK/PD modeling. Our work serves as an exemplary model for the utility of PBPK modeling to determine tissue concentrations that can be correlated to *in vitro* PD data to make meaningful predictions about drug efficacy. Furthermore, linking the model predictions with safety data is necessary when dose adjustments are being considered. We also believe that this timely report will help to guide treatment strategy against the rapidly evolving SARS-CoV-2 pandemic. This is particularly important as there are currently over 10 clinical trials worldwide investigating the efficacy of lopinavir/ritonavir against COVID-19. We envisage greater adoption of PBPK modeling for evaluating anti-infectives against SARS-CoV-2 and other diseases in the future.

SUPPORTING INFORMATION

Supplementary information accompanies this paper on the *Clinical Pharmacology & Therapeutics* website (www.cpt-journal.com).

ACKNOWLEDGMENTS

The authors thank Drs. Venkateshan Srirangam Prativadibhankara and Andrea Kwa for helpful discussions on the clinical pharmacology of lopinavir/ritonavir.

FUNDING

This research was supported by the Agency for Science, Technology and Research (A*STAR) under its Industry Alignment Fund – Pre-Positioning Programme (IAF-PP) grant number H18/01/a0/J14 as part of the A*STAR Innovations in Food and Chemical Safety (IFCS) Programme (to J.C.Y.C.). S.P.F.T. is supported by the A*STAR Graduate Academy.

CONFLICT OF INTEREST

The authors declared no competing interests for this work.

AUTHOR CONTRIBUTIONS

A.T., S.P.F.T., and J.C.Y.C. wrote the manuscript. J.C.Y.C. designed the research. A.T. and S.P.F.T. performed the research. A.T., S.P.F.T., and J.C.Y.C. analyzed the data. A.T., S.P.F.T., and J.C.Y.C. contributed new reagents/analytical tools.

© 2020 The Authors *Clinical Pharmacology & Therapeutics* © 2020 American Society for Clinical Pharmacology and Therapeutics

1. World Health Organization Coronavirus disease 2019 Situation Report 167. (2020) <<https://www.who.int/emergencies/diseases/novel-coronavirus-2019>>.
2. Centre for Drug Evaluation and Research FDA Kaletra Clinical Pharmacology and Biopharmaceutical Review. (2000) <http://www.accessdata.fda.gov/drugsatfda_docs/nda/2000/21-226_Kaletra_biopharmr_P1.pdf>.
3. Chu, C.M. *et al.* Role of lopinavir/ritonavir in the treatment of SARS: initial virological and clinical findings. *Thorax* **59**, 252–256 (2004).

4. De Wilde, A.H. *et al.* Screening of an FDA-approved compound library identifies four small-molecule inhibitors of Middle East respiratory syndrome coronavirus replication in cell culture. *Antimicrob. Agents Chemother.* **58**, 4875–4884 (2014).
5. WHO “Solidarity” clinical trial for COVID-19 treatments. (2020) <<https://www.who.int/emergencies/diseases/novel-coronavirus-2019/global-research-on-novel-coronavirus-2019-ncov/solidarity-clinical-trial-for-covid-19-treatments>>.
6. Cao, B. *et al.* A trial of lopinavir-ritonavir in adults hospitalized with severe covid-19. *N. Engl. J. Med.* **382**, 1787–1799 (2020).
7. Kirby, B.J. *et al.* Complex drug interactions of HIV protease inhibitors 2: in vivo induction and in vitro to in vivo correlation of induction of cytochrome P450 1A2, 2B6, and 2C9 by ritonavir or nelfinavir. *Drug Metab. Dispos.* **39**, 2329–2337 (2011).
8. Wagner, C. *et al.* Physiologically based pharmacokinetic modeling for predicting the effect of intrinsic and extrinsic factors on darunavir or lopinavir exposure coadministered with ritonavir. *J. Clin. Pharmacol.* **57**, 1295–1304 (2017).
9. Barter, Z.E., Tucker, G.T. & Rowland-Yeo, K. Differences in cytochrome P450-mediated pharmacokinetics between Chinese and Caucasian populations predicted by mechanistic physiologically based pharmacokinetic modelling. *Clin. Pharmacokinet.* **52**, 1085–1100 (2013).
10. Du, X. *et al.* A review of clinical pharmacokinetic and pharmacodynamic profiles of select antiretrovirals: focus on differences among Chinese patients. *Pharmacotherapy* **39**, 1179–1189 (2019).
11. López Aspiroz, E. *et al.* Population pharmacokinetics of lopinavir/ritonavir (Kaletra) in HIV-infected patients. *Ther. Drug Monit.* **33**, 573–582 (2011).
12. Smith, P.F., Dodds, M., Bentley, D., Yeo, K. & Rayner, C. Dosing will be a key success factor in repurposing antivirals for COVID-19. *Br. J. Clin. Pharmacol.* <https://doi.org/10.1111/bcp.14314>. [epub ahead of print].
13. Kumar, G.N. *et al.* Metabolism and disposition of the HIV-1 protease inhibitor lopinavir (ABT-378) given in combination with ritonavir in rats, dogs, and humans. *Pharm. Res.* **21**, 1622–1630 (2004).
14. Sham, H.L. *et al.* ABT-378, a highly potent inhibitor of the human immunodeficiency virus protease. *Antimicrob. Agents Chemother.* **42**, 3218–3224 (1998).
15. Hickman, D. *et al.* Estimation of serum-free 50-percent inhibitory concentrations for human immunodeficiency virus protease inhibitors lopinavir and ritonavir. *Antimicrob. Agents Chemother.* **48**, 2911–2917 (2004).
16. Norio, Y., Shutoku, M., Tyuji, H. & Naoki, Y. Nelfinavir inhibits replication of severe acute respiratory syndrome coronavirus 2 in vitro. *BioRxiv.* <https://doi.org/10.1101/2020.04.06.026476>. [epub ahead of print].
17. Ohashi, H. *et al.* Multidrug treatment with nelfinavir and cepharanthine against COVID-19. *BioRxiv.* <https://doi.org/10.1101/2020.04.14.03992>. [epub ahead of print].
18. Ryu, S. *et al.* Evaluation of fraction unbound across 7 tissues of 5 species. *J. Pharm. Sci.* **109**, 1178–1190 (2020).
19. Kumar, G.N., Rodrigues, A.D., Buko, A.M. & Denissen, J.F. Cytochrome P450-mediated metabolism of the HIV-1 protease inhibitor ritonavir (ABT-538) in human liver microsomes. *J. Pharmacol. Exp. Ther.* **277**, 423–431 (1996).
20. Kaspera, R. *et al.* Investigating the contribution of CYP2J2 to ritonavir metabolism in vitro and in vivo. *Biochem. Pharmacol.* **91**, 109–118 (2014).
21. Fukushima, K. *et al.* Time-dependent interaction of ritonavir in chronic use: the power balance between inhibition and induction of p-glycoprotein and cytochrome P450 3A. *J. Pharm. Sci.* **102**, 2044–2055 (2013).
22. La Porte, C.J.L. *et al.* Pharmacokinetics of adjusted-dose lopinavir-ritonavir combined with rifampin in healthy volunteers. *Antimicrob. Agents Chemother.* **48**, 1553–1560 (2004).
23. Schöller-Gyüre, M. *et al.* Steady-state pharmacokinetics of etravirine and lopinavir/ritonavir melt extrusion formulation, alone and in combination, in healthy HIV-negative volunteers. *J. Clin. Pharmacol.* **53**, 202–210 (2013).
24. Jackson, A. *et al.* Pharmacokinetics of plasma lopinavir/ritonavir following the administration of 400/100 mg, 200/150 mg and 200/50 mg twice daily in HIV-negative volunteers. *J. Antimicrob. Chemother.* **66**, 635–640 (2011).
25. Yang, W., Xiao, Q., Wang, D., Yao, C. & Yang, J. Evaluation of pharmacokinetic interactions between long-acting HIV-1 fusion inhibitor albuvirtide and lopinavir/ritonavir, in HIV-infected subjects, combined with clinical study and simulation results. *Xenobiotica* **47**, 133–143 (2017).
26. Penzak, S.R. *et al.* Echinacea purpurea significantly induces cytochrome P450 3A activity but does not alter lopinavir-ritonavir exposure in healthy subjects. *Pharmacotherapy* **30**, 797–805 (2010).
27. Eron, J.J. *et al.* Once-daily versus twice-daily lopinavir/ritonavir in antiretroviral-naïve HIV-positive patients: a 48-week randomized clinical trial. *J. Infect. Dis.* **189**, 265–272 (2004).
28. de Kanter, C.T.M.M., Colbers, E.P.H., Fillekes, Q., Hoitsma, A. & Burger, D.M. Pharmacokinetics of two generic co-formulations of lopinavir/ritonavir for HIV-infected children: a pilot study of paediatric lopimmune versus the branded product in healthy adult volunteers. *J. Antimicrob. Chemother.* **65**, 538–542 (2010).
29. Bierman, W.F.W. *et al.* Protease inhibitors atazanavir, lopinavir and ritonavir are potent blockers, but poor substrates, of ABC transporters in a broad panel of ABC transporter-overexpressing cell lines. *J. Antimicrob. Chemother.* **65**, 1672–1680 (2010).
30. Liu, L. & Unadkat, J.D. Interaction between HIV protease inhibitors (PIs) and hepatic transporters in sandwich cultured human hepatocytes: implication for PI-based DDIs. *Biopharm. Drug Dispos.* **34**, 155–164 (2013).
31. Smith, D.A., Di, L. & Kerns, E.H. The effect of plasma protein binding on in vivo efficacy: misconceptions in drug discovery. *Nat. Rev. Drug Discov.* **9**, 929–939 (2010).
32. Twigg, H.L. *et al.* Measurement of antiretroviral drugs in the lungs of HIV-infected patients. *HIV Ther.* **4**, 247–251 (2010).
33. Atzori, C., Villani, P., Regazzi, M., Maruzzi, M. & Cargnel, A. Detection of intrapulmonary concentration of lopinavir in an HIV-infected patient. *AIDS* **17**, 1710–1711 (2003).
34. Chu, X. *et al.* Intracellular drug concentrations and transporters: Measurement, modeling, and implications for the liver. *Clin. Pharmacol. Ther.* **94**, 126–141 (2013).
35. Jeon, S. *et al.* Identification of antiviral drug candidates against SARS-CoV-2 from FDA-approved drugs. *bioRxiv.* <https://doi.org/10.1101/2020.03.20.999730>. [epub ahead of print].
36. Choy, K.T. *et al.* Remdesivir, lopinavir, emetine, and homoharringtonine inhibit SARS-CoV-2 replication in vitro. *Antiviral Res.* **178**, 104786 (2020).
37. Hoffmann, M. *et al.* SARS-CoV-2 cell entry depends on ACE2 and TMPRSS2 and is blocked by a clinically proven protease inhibitor. *Cell* **181**, 271–280.e8 (2020).
38. Matsuyama, S. *et al.* Enhanced isolation of SARS-CoV-2 by TMPRSS2-expressing cells. *Proc. Natl. Acad. Sci. USA* **117**, 7001–7003 (2020).
39. World Health Organization (WHO). WHO discontinues hydroxychloroquine and lopinavir/ritonavir treatment arms for COVID-19. (2020) <<https://www.who.int/news-room/detail/04-07-2020-who-discontinues-hydroxychloroquine-and-lopinavir-ritonavir-treatment-arms-for-covid-19>>.
40. Podzamczar, D. *et al.* High-dose lopinavir/ritonavir in highly treatment-experienced HIV-1 patients: efficacy, safety, and predictors of response. *HIV Clin. Trials* **8**, 193–204 (2007).
41. Vicente, J. *et al.* Assessment of multi-ion channel block in a phase I randomized study design: results of the CiPA phase I ECG biomarker validation study. *Clin. Pharmacol. Ther.* **105**, 943–953 (2019).
42. Maisch, B. SARS-CoV-2 as potential cause of cardiac inflammation and heart failure. Is it the virus, hyperinflammation, or MODS? *Herz* **45**, 321–322 (2020).
43. Huang, S.M. *et al.* Therapeutic protein-drug interactions and implications for drug development. *Clin. Pharmacol. Ther.* **87**, 497–503 (2010).
44. World Health Organization (WHO). International clinical trials registry platform (2020) <<https://www.who.int/ictrp/en/>>.